PROCEEDINGS OF SCIENCE

Performance of an array of $6 \times 6 \times 20\,mm^3$ virtual Frisch-grid CdZnTe detectors with a waveform sampling readout system

Makoto Sasaki,[a,e,*] **Aleksey E. Bolotnikov,**[b] **Nicholas W. Cannady,**[c,e] **Gabriella A. Carini,**[b] **Sven C. Herrmann,**[b] **John W. Mitchell,**[d] **Alexander A. Moiseev**[a,e] **and Lucas D. Smith**[a]

[a] *University of Maryland College Park, College Park, MD 20742, U.S.A.*
[b] *Brookhaven National Laboratory, Upton, NY 11973, U.S.A.*
[c] *University of Maryland Baltimore County, Baltimore, MD 21250, U.S.A.*
[d] *NASA Goddard Space Flight Center, Greenbelt, MD 20771, U.S.A.*
[e] *Center for Research and Exploration in Space Science and Technology, NASA/GSFC Greenbelt, MD 20771, U.S.A*

E-mail: Makoto.Sasaki@nasa.gov

Arrays of CdZnTe (CZT) bars with high spatial and energy resolution are an enabling technology for future space missions, such as the image plane detector of the Galactic Explorer with a Coded Aperture Mask Compton Telescope (GECCO). GECCO will explore the medium-energy (100 keV–10 MeV) γ-ray sky, which is among the least covered windows to the Universe with a massive potential for discovery. We have integrated an array of $6 \times 6 \times 20\,mm^3$ virtual Frisch-grid (VFG) CZT detectors, measuring signals from the cathodes, anodes, and pads on each of the four sides of each bar. The VFG CZT detector is read out with an IDEAS GDS-100 waveform sampling readout system to optimize the signal processing and event reconstruction. We evaluated the energy and position resolution of the integrated VFG CZT array with a ^{137}Cs source and successfully demonstrated better than 1% energy resolution and finer than 1 mm position resolution at 662 keV. Furthermore, we carried out a beam test at the High Intensity Gamma-ray Source (HIGS) at Duke University to investigate the performance of the system for higher energy γ-rays. Together with the basic performance obtained from the ^{137}Cs source, we present here those results from the beam test with various γ-ray energies up to 8 MeV.

38th International Cosmic Ray Conference (ICRC2023)
26 July - 3 August, 2023
Nagoya, Japan

ICRC2023
38th International Cosmic Ray Conference
The Astroparticle Physics Conference

*Speaker

PoS(ICRC2023)761

1. Introduction

Although the precise observation of γ-ray spectra is important for understanding our universe, not all energy regions have been observed with the same sensitivity. Of particular note is the energy range from 100 keV to 10 MeV, for which the sensitivity of available measurements is one to two orders of magnitude lower than other regions. This is due to the difficulty of the measurement itself, as Compton scattering events and pair producing events have very different signatures in a detector. Several experiment concepts are being developed to explore the medium energy γ-ray sky, including the Galactic Explorer with a Coded Aperture Mask Compton Telescope (GECCO). [1].

GECCO is a unique concept of combined dual mode γ-ray Compton telescope with coded aperture mask. It will conduct high-sensitivity measurements of the cosmic γ-radiation in the energy range from 100 keV to $\sim$ 10 MeV and create intensity maps with high spectral and spatial resolution, focusing on sensitive separation of diffuse and point-source components. GECCO utilizes a novel CZT Imaging Calorimeter as a standalone Compton Telescope and as a focal-plane detector. A coded aperture mask modulates the incident photon flux and creates an image on the CZT detector plane. The mask is deployable and can be placed at a large distance from the detector for high-angular resolution.

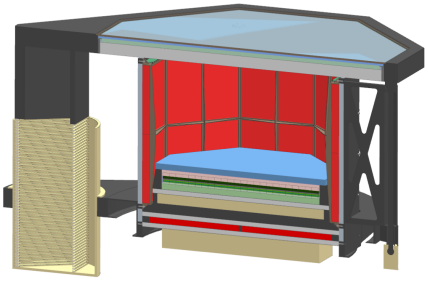

Figure 1: GECCO Instrument cross-sectional view.

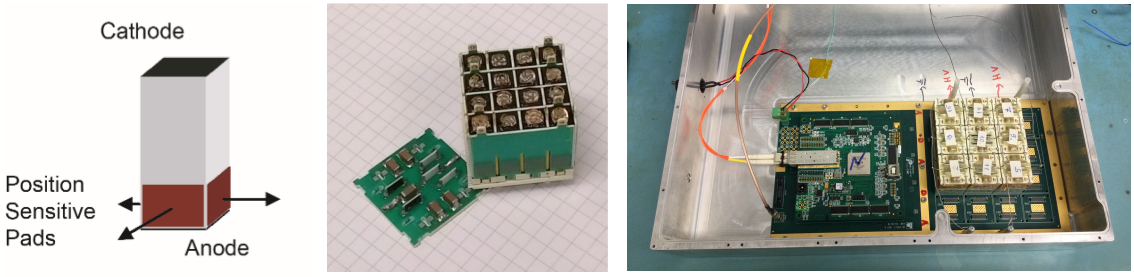

(a) (b) (c)

Figure 2: a) A schematic drawing of the position-sensitive VFG CZT detector, b) A custom-made crate with 4×4 CZT bars, c) A photo of the CZT Imaging Calorimeter with 3×3 crates for the ComPair instrument.

The virtual Frisch-Grid (VFG) CZT detector [2] developed by BNL group has been adopted for the GECCO CZT Imaging Calorimeter. Copper pads placed near the anode screen out the induced signal from slow moving positive holes such that only the electrons passing through the grid generates the signal on the anode. This screening means that the position dependence on the anode signal is effectively suppressed and that the anode signal is related only to the energy deposited in the crystal. The relative signals induced on the pads are used to determine the X- and Y-positions of the interaction point, and the timing information or the ratio of the cathode signal to the anode signal is used to determine the Z-position. The dimensions of the CZT bars reported on in this work are 6 mm × 6 mm × 20 mm, and 16 such CZT bars are arranged into each crate as a 4×4 array (Figure 2 a, b). The crates can be installed on a motherboard of any required geometry

depending on the detector design. The CZT Imaging Calorimeter for the ComPair instrument [3] is shown on Figure 2 c, where the crates are arranged in a 3×3 array to cover a 90 mm × 90 mm active area.

2. Detectors and readout electronics

We have evaluated the performance of the CZT Imaging Calorimeter using the recently developed IDEAS GDS-100 readout system with an IDM-121 waveform sampling ASIC (Figure 3). The IDM-121 has 121 (+2 special) input channels, each channel having a pre-amplifier which is connected to a 160-cell analog pipeline. The analog pipeline is used as a ring buffer, and the signal from the pre-amplifier is continuously sampled into the pipeline until readout is triggered. Up to four IDM-121s can be installed on the GDS-100 motherboard, covering an active area of up to 64 mm × 64 mm with the current crate design.

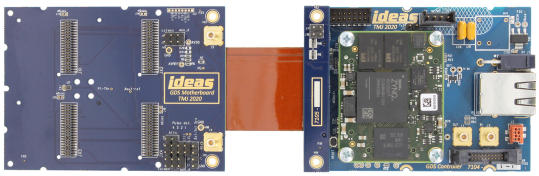

Figure 3: IDEAS GDS-100 system. The motherboard with 4 connectors for IDM-121 is on the left side and the control board is on the right side interconnected by a flex circuit.

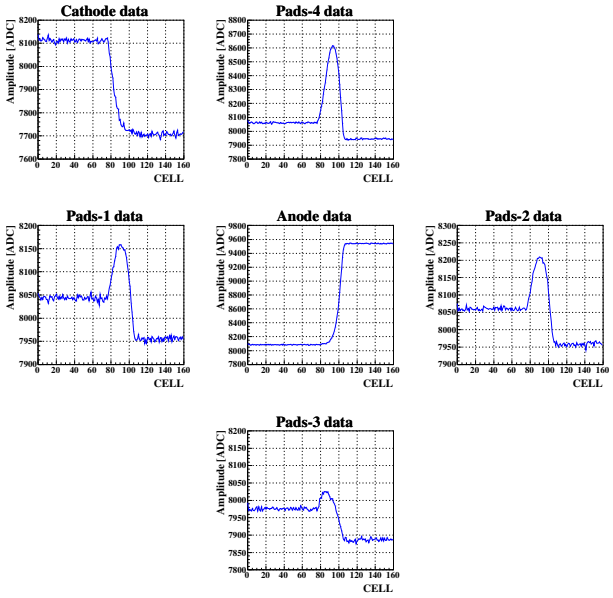

Figure 4: Waveforms captured by GDS-100 system for a ^{137}Cs event in a CZT bar.

Figure 4 shows waveforms captured by the GDS-100 system for a ^{137}Cs event in a CZT bar. The central panel shows the anode signal waveform, and the 4 pad signals are plotted above, below, left, and right of it. The top left plot is the cathode signal waveform. The deposited energy is determined from the anode signal and the 3D interaction position is determined from the 4 pad signals and the cathode to anode ratio as described in the previous section.

A GUI-based DAQ program was developed using the CERN ROOT package [4] to control GDS-100 system. The CZT data digitized by the IDM-121s are read by the control board equipped with an FPGA and sent to the DAQ computer as a UDP packet via Ethernet cable. The GDS-100 system is controlled by sending a TCP packet from the DAQ computer to the control board which contains control codes. Figure 5 is a screenshot of the GUI control panel actually in operation during the HIGS beam test. The detector performance can be monitored with the histograms of the processed anode signals, as shown on the right pane of the GUI panel for one of the 16-bar crates. The beam energy at the time of this screenshot was 5 MeV and the diameter

of the beam profile was about 6 mm, which corresponds to the cross-sectional size of a CZT bar. We adjusted the position of the detector so that the beam center matched the center of one of the CZT bar. The target bar can be easily identified on the plots (second from the left and second from the top). The 511 keV positron annihilation line is seen in the neighboring bars, corresponding to the detection of the escaping positron occuring in the pair-production interaction of the incident photon, starting at its energy above 1,022 keV.

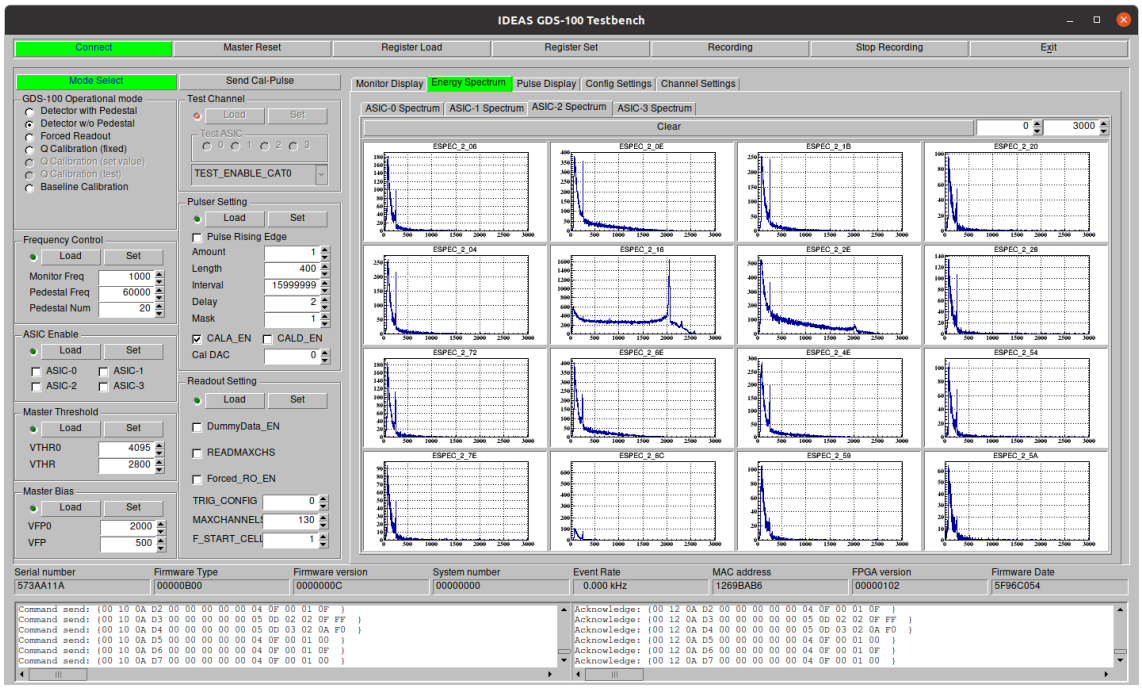

Figure 5: A screenshot of the GDS-100 control GUI panel.

3. Data analysis and detector performances

3.1 Baseline correction

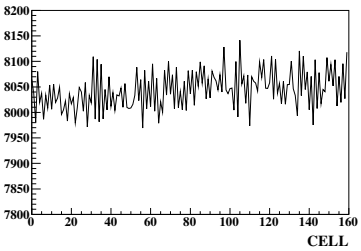

(a) Baseline data for one ASIC input channel

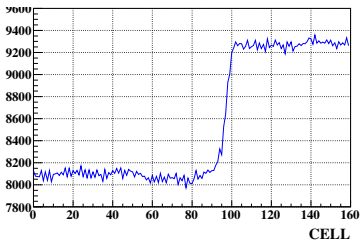

(b) Amplitude data for an anode signal before the baseline correction

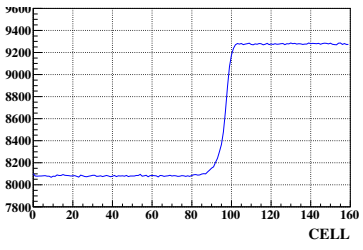

(c) Amplitude data for an anode signal after the baseline correction

Figure 6: Example of the Baseline correction, applied for an anode signal

The 160-cell analog pipeline connected to the pre-amplifier has a different baseline in each cell due to process variations in the hardware. Figure 6a shows a measurement of the baseline

of the analog pipeline, Figure 6b shows a waveform captured on the pipeline before the baseline correction, and Figure 6c shows the same waveform after the baseline correction.

3.2 Depth correction

The ratio of the cathode signal to the anode signal correlates well with the Z-position of the γ-ray interaction. Although the position dependence of the output anode signal, which carries the energy information, is suppressed by the Frisch-grid design, some remains due to shielding inefficiency of the virtual grid and to crystal non-uniformity. Therefore, to improve the energy resolution, the magnitude of the anode signal needs to be corrected by the depth of interaction, which can be estimated from the Cathode to Anode signal ratio, as shown in Figure 7.

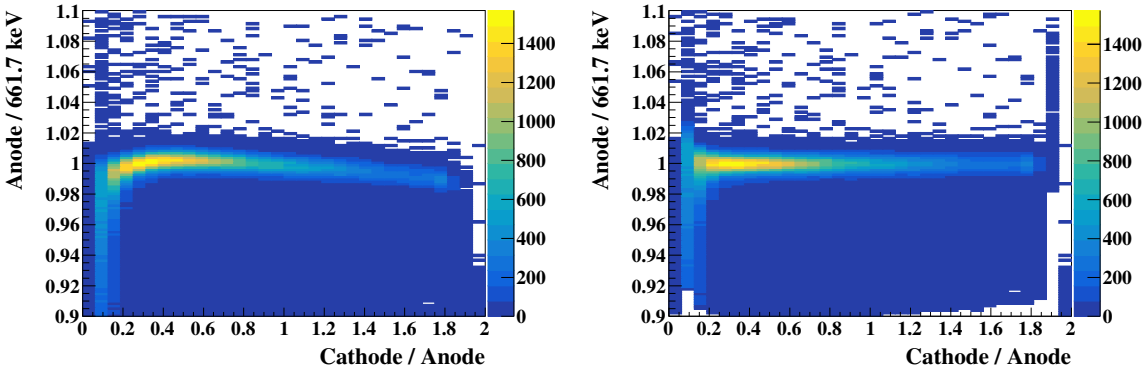

(a) Before applying the depth correction

(b) After applying the depth correction

Figure 7: A cross plot of the Anode/661.7keV vs. Cathode/Anode for ^{137}Cs data a) before applying the depth correction, b) after applying the depth correction

3.3 Energy resolution

We used ^{137}Cs source to determine the energy resolution of the system. The spectrum from one CZT bar is shown in Figure 8a along with the distribution of the energy resolution from two crates (32 bars, Figure 8b). The peak value of the energy resolution distribution was less than 1%.

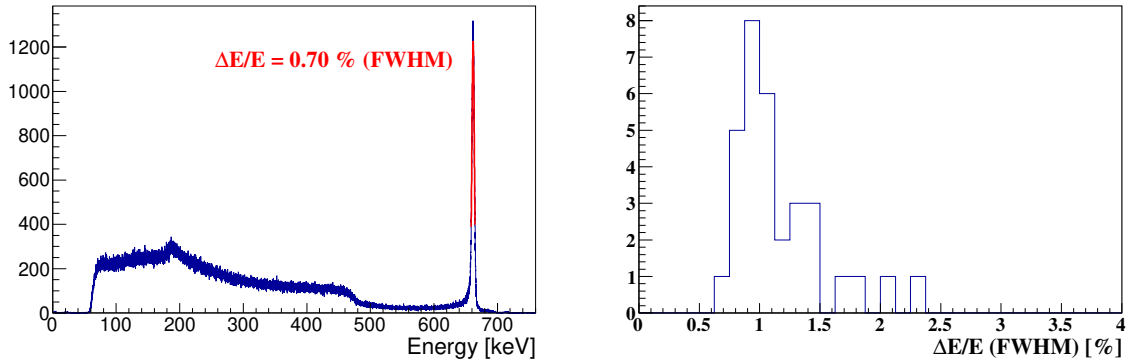

(a) ^{137}Cs energy spectrum from a CZT bar. ΔE/E is 0.7% (FWHM)

(b) The energy resolution distribution from two crates (32 bars). The peak of the distribution is less than 1%

Figure 8: The energy resolution of the CZT Imaging Calorimeter determined using ^{137}Cs.

3.4 Position resolution

To determine the position resolution, we used ^{137}Cs source and a tungsten collimator with a 0.08 mm gap. Figure 9a shows the reconstructed hit map of the detected events. Figure 9b shows the best linear fit line in red color, and Figure 9c shows the residual distance distribution between the reconstructed hit location and the fit line. As we expected, we obtained a position resolution (FWHM) for the system better than 1 mm.

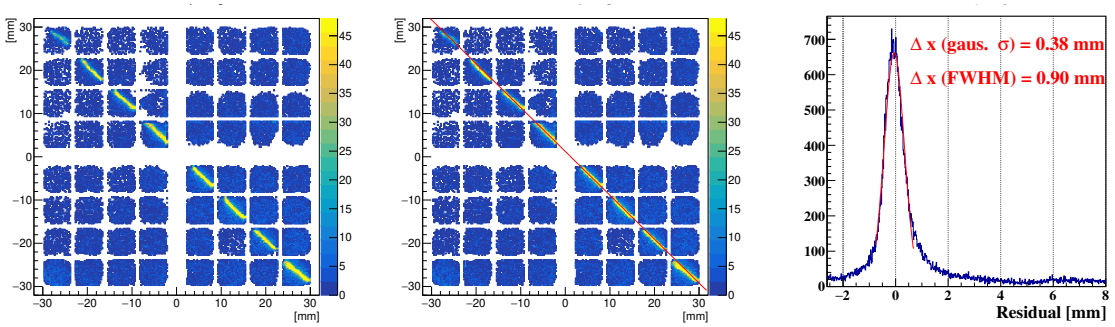

(a) ^{137}Cs hit map with collimator with 0.08 mm gap

(b) ^{137}Cs hit map with the best fit line shown in red

(c) ^{137}Cs hit residual distance from the fitted line

Figure 9: Position resolution of the CZT Imaging Calorimeter determined with the use of ^{137}Cs source and a tungsten collimator with 0.08 mm gap

4. HIGS beam test

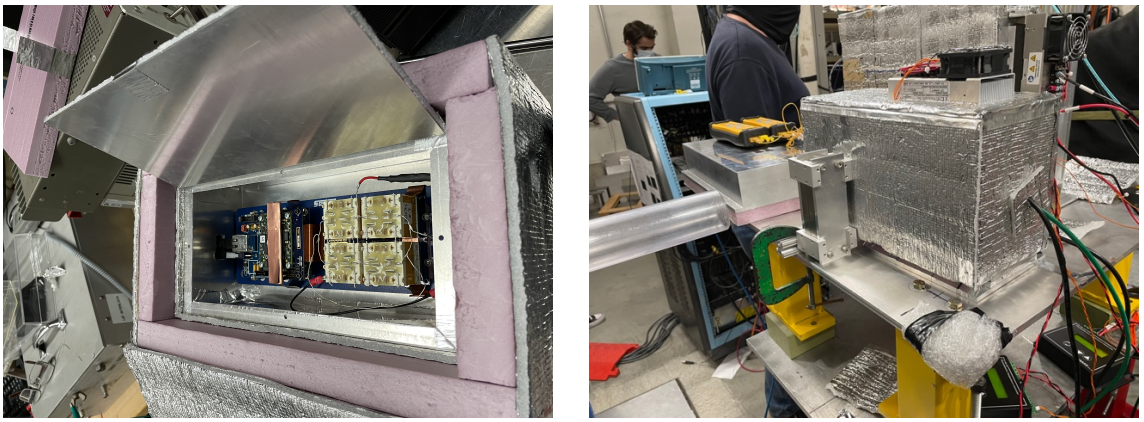

(a) Test detector with multi-layer thermal shield to keep the temperature stable during the test

(b) Test detector at the beam line. A Peltier cooler was attached on the top of the aluminum box

Figure 10: Photos taken at the HIGS beam test.

We carried out the beam test at the Triangle University Nuclear Laboratory / High Intensity Gamma-ray Source (TUNL/HIGS) at Duke University on November 1–5, 2021 with total 20 hours of actual beam time to evaluate the performance of the CZT detectors with IDEAS readout system in the energy range from 2 MeV to 8 MeV. The test CZT detector we used at the beam is shown in

Figure 10. The GDS-100 system was installed in the small aluminum box with multiple thermal shields (Figure 10a) to keep the temperature stable during the beam test and to reduce the internal moisture condensation on the high-voltage paths and on the CZT bars themself. 4 CZT crates were used in this test, as a maximum what can be handled by a single GDS-100 system. A copper heat strap was attached to the FPGA on the control board for efficient cooling, and a Peltier cooler (CP-040HT, TE technology, Inc.) was attached to the top of the aluminum box to control the temperature inside the box as shown in Figure 10b. We kept the temperature around 18–20 degrees C during the beam test. A tungsten collimator was located at the front of the test detector to evaluate the position resolution of the detector. A HV cable, Ethernet cable, and power cable were connected to the detector through holes on the side wall.

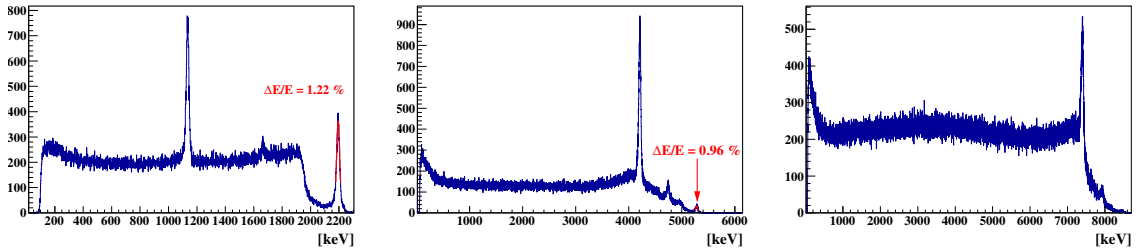

(a) 2.1MeV, Single bar **(b)** 5 MeV, Single bar **(c)** 8 MeV, Single bar

(d) 2.1 MeV, All bars **(e)** 5 MeV, All bars **(f)** 8 MeV, All bars

Figure 11: Energy spectra for various γ-ray beam energies from a single CZT bar in the beam (a)(b)(c) and from all CZT bars (d)(e)(f)

Energy spectra with various γ-ray beam energies obtained at the HIGS beam test are shown in Figure 11. The upper figures (11a),(11b),(11c) show energy spectra from the single CZT bar targeted by the beam, and the bottom figures (11d),(11e),(11f) show energy spectra after summing the signals from all CZT bars. There are clear 511 keV lines in the bottom figures for 5 and 8 MeV, which appear to have come from photons which create an electron-positron pair outside of the detector. The energy resolution of the CZT bars at the beam energy was obtained from a Gaussian fit for the 2.1 MeV and 5 MeV runs. There were too few events that absorbed all the beam energy for the 8 MeV. ΔE/E (FWHM) at the full absorption peak for the 5MeV beam was 0.96%. The energy resolution of the beam itself has been measured separately and is estimated to be about 0.6%, so the energy resolution of the instrument itself is therefore estimated to be 0.7%, which is consistent with the energy resolution confirmed in the laboratory using radioactive sources.

5. Summary

We have evaluated the performance of the CZT Imaging Calorimeter with the IDEAS GDS-100 waveform sampling readout system. The obtained energy resolution (ΔE/E (FWHM)) for the energy range from 600 keV to 5 MeV was found to be better than 1%, and the position resolution of the system (FWHM) was found to be better than 1 mm with a ^{137}Cs source. The performance was confirmed at the HIGS beam test for higher energies. We are currenty investigating the performance of a larger size CZT bar (8 mm × 8 mm × 32 mm) for use in higher energy γ-ray observation and for increase of the active area of the Imaging Calorimeter [5].

Acknowledgments

This work was supported by NASA/APRA award 80NSSC20K0573. The CRESST/GSFC team members were supported by NASA award 80GSFC21M0002. The team is grateful to the IDEAS leadership and engineers (Aage Kalsæg, Gunnar Mæhlum, Tor Magnus Johansen, and others) and to the TUNL/HIGS scientists and engineers (Ying Wu, Calvin Howell, Stepan Mikhailov, and others) for their invaluable support in the instrument development and testing.

References

[1] E. Orlando, E. Bottacini, A. Moiseev, A. Bodaghee, W. Collmar, T. Ensslin, I. V. Moskalenko, M. Negro, S. Profumo, S. W. Digel, et al., *Exploring the MeV sky with a combined coded mask and Compton telescope: the Galactic Explorer with a Coded aperture mask COmpton telescope (GECCO)*, *Journal of Cosmology and Astroparticle Physics* **2022** (2022), no. 07 036.

[2] A. Bolotnikov, G. Camarda, G. De Geronimo, J. Fried, D. Hodges, A. Hossain, K. Kim, G. Mahler, L. O. Giraldo, E. Vernon, et al., *A 4× 4 array module of position-sensitive virtual Frisch-grid CdZnTe detectors for gamma-ray imaging spectrometers*, *Nuclear Instruments and Methods in Physics Research Section A: Accelerators, Spectrometers, Detectors and Associated Equipment* **954** (2020) 161036.

[3] D. Shy, C. Kierans, N. Cannady, R. Caputo, S. Griffin, E. Grove, E. Hays, E. Kong, N. Kirschner, I. Liceaga-Indart, et al., *Development of the ComPair gamma-ray telescope prototype*, in *Space Telescopes and Instrumentation 2022: Ultraviolet to Gamma Ray*, vol. 12181, pp. 622–635, SPIE, 2022.

[4] R. Brun and F. Rademakers, *ROOT—An object oriented data analysis framework*, *Nuclear instruments and methods in physics research section A: accelerators, spectrometers, detectors and associated equipment* **389** (1997), no. 1-2 81–86.

[5] A. Bolotnikov, G. Carini, A. Dellapenna, J. Fried, G. Deptuch, J. Haupt, S. Herrmann, P. Maj, A. Moiseev, et al., *Development of position-sensitive CdZnTe arrays for gamma-ray telescopes*, *2022 IEEE Nuclear Science Sysposium, Medical Imaging Conference, and Room-Temeperature Semiconductor Detectors Conference* (2022).